

Design of Perfect Reconstruction QMF Banks by A Null-Space Projection Method

H. Xu, W.-S. Lu, and A. Antoniou

Department of Electrical and Computer Engineering
University of Victoria
Victoria, B.C., Canada, V8W 3P6

Email: hxu@ece.uvic.ca, wslu@ece.uvic.ca, and andreas@ece.uvic.ca

ABSTRACT

A new method is proposed for the design of two-channel linear-phase perfect reconstruction QMF banks. The analysis lowpass filter is first designed by a conventional method, and then the synthesis lowpass filter is obtained by using a null-space projection approach. This method is then extended to the design of two-channel perfect reconstruction QMF banks with low reconstruction delay, which are desirable in some applications. Two design examples are given to illustrate the proposed methods.

I. INTRODUCTION

The importance of quadrature-mirror-filter (QMF) banks in subband coding has been widely recognized. Since the quadrature mirror structure leads to complete cancellation of interband aliasing due to the overlapping filter responses, the design is reduced to satisfying the perfect reconstruction condition while minimizing the intra-band aliasing. Since the mid 70's several approaches have been proposed for the design of QMF banks [1]-[4]. Some of the design methods lead to near-perfect reconstruction QMF banks [1][2] while others lead to perfect-reconstruction QMF banks [3][4].

In this paper, a new method for the design of linear-phase perfect reconstruction QMF banks is proposed on the basis of a time-domain formulation. The analysis lowpass filter is first obtained by a conventional method and the synthesis lowpass filter is obtained by a null-space projection approach. The proposed method is then extended to the design of low-delay perfect reconstruction QMF banks which are useful in applications where long reconstruction delays are undesirable. Two design examples are presented to demonstrate the performance of the QMF banks obtained.

The authors are grateful to Micronet, Networks of Centres of Excellence Program, and the Natural Science and Engineering Research Council of Canada for supporting this work.

II. DESIGN METHOD

A. Design of Linear-Phase Perfect Reconstruction QMF Banks

Consider the two-channel filter bank shown in Fig. 1. The output and input relations of the system are given by

$$\hat{X}(z) = \frac{1}{2}[H_0(z)G_0(z) + H_1(z)G_1(z)] \cdot X(z) + \frac{1}{2}[H_0(-z)G_0(z) + H_1(-z)G_1(z)] \cdot X(-z) \quad (1)$$

where the second term on the right side represents the aliasing. By assuming that $G_1(z) = -H_0(-z)$, $H_1(z) = G_0(-z)$, the aliasing term is cancelled and (1) becomes

$$\hat{X}(z) = \frac{1}{2}[H_0(z)G_0(z) - H_0(-z)G_0(-z)]X(z) \quad (2)$$

To reconstruct the output perfectly, it is required that

$$H_0(z)G_0(z) - H_0(-z)G_0(-z) = z^{-k_d} \quad (3)$$

where k_d is the system delay. If we assume that the coefficients of $H_0(z)$ and $G_0(z)$ are symmetrical and their lengths, N and M , are even, $M > N$, and $N + M$ is a multiple of 4, then it can be readily shown that k_d in (3) is equal to $(M + N)/2 - 1$.

In the time domain, (3) can be expressed as

$$\mathbf{H}\mathbf{g} = \mathbf{m} \quad (4)$$

where

$$\mathbf{H} = 2 \left[\mathbf{b}_1 + \mathbf{b}_M \quad \mathbf{b}_2 + \mathbf{b}_{M-1} \quad \cdots \quad \mathbf{b}_{\frac{M}{2}} + \mathbf{b}_{\frac{M}{2}+1} \right]$$

$$\mathbf{B} = \left[\mathbf{b}_1 \quad \mathbf{b}_2 \quad \cdots \quad \mathbf{b}_M \right]$$

$$= \begin{bmatrix} h(1) & h(0) & 0 & \cdots & \cdots & 0 \\ h(3) & h(2) & h(1) & h(0) & \cdots & 0 \\ \vdots & \vdots & \vdots & \vdots & \vdots & \vdots \\ h(N-1) & h(N-2) & \cdots & \cdots & \cdots & 0 \\ 0 & 0 & h(N-1) & \cdots & \cdots & 0 \\ \vdots & \vdots & \vdots & \vdots & \vdots & \vdots \end{bmatrix}$$

$$\mathbf{g} = [g(0) \ g(1) \ \cdots \ g(M/2 - 1)]^T$$

$$\mathbf{m} = [0 \ \cdots \ 0 \ 1]^T \in \mathbf{R}^{\frac{M+N}{4} \times 1}$$

$h(n)$, for $n = 0, \dots, N - 1$ is the impulse response of filter \mathbf{H}_0 , and $g(n)$, for $n = 0, \dots, M/2 - 1$ is the first half of the impulse response of filter G_0 . In our approach, \mathbf{H}_0 is first designed by a conventional FIR filter design method; then the entries of \mathbf{g} are obtained by solving the linear system of equations in (4), where we have $(M+N)/4$ equations and $M/2$ unknowns. This leads to the number of degrees of freedom

$$f_d = \frac{M}{2} - \frac{M+N}{4} = \frac{M-N}{4} \quad (5)$$

As is well known, the general solution of (4) is given by

$$\mathbf{g} = \mathbf{H}^\dagger \mathbf{m} + (\mathbf{I} - \mathbf{H}^\dagger \mathbf{H}) \boldsymbol{\phi} \quad (6)$$

where \mathbf{H}^\dagger is the Moore-Penrose pseudo-inverse of \mathbf{H} , and $\boldsymbol{\phi}$ is an arbitrary column vector. Note that

$$\mathbf{H}(\mathbf{I} - \mathbf{H}^\dagger \mathbf{H}) \boldsymbol{\phi} = 0$$

i.e., the second term on the right side of (6) represents a vector in the null space of \mathbf{H} . In other words, $(\mathbf{I} - \mathbf{H}^\dagger \mathbf{H}) \boldsymbol{\phi}$ projects an arbitrary vector $\boldsymbol{\phi}$ onto the null space of \mathbf{H} . Let

$$\mathbf{H} = \mathbf{U} \begin{bmatrix} \sigma_1 & & & 0 & \cdots & 0 \\ & \ddots & & \vdots & & \vdots \\ & & \sigma_{\frac{M+N}{4}} & 0 & \cdots & 0 \end{bmatrix} \mathbf{V}^T \quad (7)$$

be the SVD decomposition of \mathbf{H} . It can be shown that \mathbf{g} in (6) can be written as

$$\mathbf{g} = \mathbf{S}_c + \mathbf{V}^* \boldsymbol{\phi}^* \quad (8)$$

where

$$\mathbf{S}_c = \mathbf{H}^\dagger \mathbf{m}$$

$$= \mathbf{V} \begin{bmatrix} \sigma_1^{-1} & & & & & \\ & \ddots & & & & \\ & & \sigma_{\frac{M+N}{4}}^{-1} & & & \\ 0 & \cdots & 0 & \sigma_{\frac{M+N}{4}}^{-1} & & \\ \vdots & & \vdots & & & \\ 0 & \cdots & 0 & & & \end{bmatrix} \mathbf{U}^T \mathbf{m}$$

$$\mathbf{V}^* = [\mathbf{v}_{\frac{M+N}{4}+1} \ \cdots \ \mathbf{v}_{\frac{M}{2}}]$$

$$\boldsymbol{\phi}^* = [\phi_1^* \ \cdots \ \phi_{\frac{M-N}{4}}^*]^T$$

\mathbf{v}_i , for $i = (M+N)/4 + 1, \dots, M/2$ is the i th column of matrix \mathbf{V} , and $\boldsymbol{\phi}^*$ contains f_d free parameters. On comparing (8) with (6), it is observed that the last f_d

column vectors of \mathbf{V}^* constitute a basis of the null space of \mathbf{H} ; hence the problem of designing G_0 amounts to finding an optimal $\boldsymbol{\phi}^*$ such that the combination of the column vectors of \mathbf{V}^* , $\mathbf{V}^* \boldsymbol{\phi}^*$, leads to the minimum of

$$E = \int_{\omega_s}^{\pi} M_g^2(\omega) d\omega$$

$$= (\mathbf{S}_c + \mathbf{V}^* \boldsymbol{\phi}^*)^T \mathbf{Q} (\mathbf{S}_c + \mathbf{V}^* \boldsymbol{\phi}^*) \quad (9)$$

where ω_s is the stopband edge of G_0 ,

$$M_g(\omega) = 2 \mathbf{g}^T \mathbf{c}(\omega)$$

$$\mathbf{c}(\omega) = [\cos(\frac{M-1}{2}\omega) \ \cdots \ \cos(\frac{1}{2}\omega)]^T$$

$$\mathbf{Q} = 4 \int_{\omega_s}^{\pi} \mathbf{c}(\omega) \mathbf{c}(\omega)^T d\omega$$

and the (i, j) th entry of \mathbf{Q} is given by

$$q_{ij} = 2 \begin{cases} \pi - \omega_s - \frac{1}{a_1} \sin a_1 \omega_s & i = j \\ -\frac{1}{a_1} \sin a_1 \omega_s - \frac{1}{a_2} \sin a_2 \omega_s & i \neq j \end{cases}$$

with $i, j = 1, \dots, M/2$, $a_1 = i + j - N - 1$, and $a_2 = i - j$. By imposing $\nabla_{\boldsymbol{\phi}^*} E = 0$, the minimum point can be obtained as

$$\boldsymbol{\phi}_{opt}^* = -(\mathbf{V}^{*T} \mathbf{Q} \mathbf{V}^*)^{-1} \mathbf{V}^{*T} \mathbf{Q} \mathbf{S}_c \quad (10)$$

and the coefficients of $G_0(z)$ can be obtained as

$$\mathbf{g}^* = \mathbf{S}_c + \mathbf{V}^* \boldsymbol{\phi}_{opt}^* \quad (11)$$

The design procedure can now be summarized as follows:

Algorithm

- Step 1** Use a conventional method to design a linear-phase, lowpass, FIR filter \mathbf{H}_0 whose length is N .
- Step 2** Form matrices \mathbf{H} and \mathbf{m} as in (4).
- Step 3** Obtain the SVD of \mathbf{H} as in (7), and calculate \mathbf{S}_c and \mathbf{Q} in (8) and (9).
- Step 4** Obtain $\boldsymbol{\phi}_{opt}^*$ using (10) and \mathbf{g}^* using (11).

B. Design of Low-Delay Perfect Reconstruction QMF Banks

The assumption of linear-phase responses for \mathbf{H}_0 and G_0 leads to fixed system delay $(M+N)/2 - 1$, which is sometimes undesirable in applications where the orders of the filters are high. If the assumption on symmetry of the coefficients in $H_0(z)$ and $G_0(z)$ is removed, then it is possible to design a filter bank with low reconstruction delay as demonstrated in [5]. We assume that the desired reconstruction delay k_d is an odd integer. The perfect reconstruction condition in (3) can be written in the time-domain as

$$\mathbf{H}_L \mathbf{G}_L = \mathbf{m}_L \quad (12)$$

where

$$\mathbf{H}_L = 2 \begin{bmatrix} h(1) & h(0) & 0 & \cdots & \cdots & 0 \\ h(3) & h(2) & h(1) & h(0) & \cdots & 0 \\ \vdots & \vdots & \vdots & \vdots & \vdots & \vdots \\ h(N-1) & h(N-2) & \cdots & \cdots & \cdots & 0 \\ 0 & 0 & h(N-1) & \cdots & \cdots & \vdots \\ \vdots & \vdots & \vdots & \vdots & \vdots & \vdots \\ 0 & \cdots & \cdots & h(N-1) & h(N-2) & \vdots \end{bmatrix}$$

$$\mathbf{g}_L = [g(0) \ g(1) \ \cdots \ g(M-1)]^T$$

$$\mathbf{m}_L = [0 \ \cdots \ 0 \ 1 \ 0 \ \cdots \ 0]^T \in \mathbf{R}^{\frac{M+N}{2}-1 \times 1}$$

where the $(k_d + 1)/2$ th entry of \mathbf{m}_L is unity. A low-pass FIR filter H_0 is first designed with group delay $k_{d1} < (N-1)/2$ and then \mathbf{g}_L is obtained by solving (12). In (12) there are $(M+N)/2 - 1$ equations and M unknowns. Hence the number of degrees of freedom in the design is

$$f_d = M - \frac{M+N}{2} + 1 = \frac{M-N}{2} + 1 \quad (13)$$

As in the design of linear-phase QMF banks described in the preceding section, the general solution of (12) is given by

$$\mathbf{g}_L = \mathbf{H}_L^\dagger \mathbf{m}_L + (\mathbf{I} - \mathbf{H}_L^\dagger \mathbf{H}_L) \phi_L$$

$$= \mathbf{S}_{cL} + \mathbf{V}_L^* \phi_L^* \quad (14)$$

where

$$\mathbf{S}_{cL} = \mathbf{H}_L^\dagger \mathbf{m}_L$$

$$\mathbf{V}_L^* = [\mathbf{v}_{\frac{M+N}{2}}^* \ \cdots \ \mathbf{v}_M^*]$$

$$\phi_L^* = [\phi_1^* \ \cdots \ \phi_{\frac{M-N}{2}+1}^*]^T$$

\mathbf{v}_i , for $i = (M+N)/2, \dots, M$, is the i th column of the right orthogonal matrix in the SVD decomposition of matrix \mathbf{H}_L , and ϕ_L^* is an arbitrary vector of dimension $(M-N)/2 + 1$.

The coefficients of the transfer function constitute vector \mathbf{g}_L^* given by (14) where parameter vector ϕ_L^* is determined by minimizing the objective function

$$E_L = \int_0^{\omega_p} |G_0(e^{j\omega}) - e^{-j\omega k_{d2}}|^2 d\omega + \int_{\omega_s}^{\pi} |G_0(e^{j\omega})|^2 d\omega$$

$$= \phi_L^{*T} (\mathbf{V}_L^{*T} \mathbf{Q}_L \mathbf{V}_L^*) \phi_L^* + 2 \phi_L^{*T} (\mathbf{V}_L^{*T} \mathbf{Q}_L \mathbf{S}_{cL} - \mathbf{V}_L^{*T} \mathbf{d}_L) + \omega_p + \mathbf{S}_{cL}^T \mathbf{Q}_L \mathbf{S}_{cL} \quad (15)$$

where

$$\mathbf{Q}_L = \begin{bmatrix} \pi + \omega_p - \omega_s & \psi(\omega_p, \omega_s, 1) & \cdots & \psi(\omega_p, \omega_s, N-1) \\ \psi(\omega_p, \omega_s, 1) & \pi + \omega_p - \omega_s & & \\ \vdots & & \ddots & \\ \psi(\omega_p, \omega_s, N-1) & \cdots & \cdots & \pi + \omega_p - \omega_s \end{bmatrix}$$

$$\psi(\omega_p, \omega_s, k) = \frac{1}{k} (\sin k\omega_p - \sin k\omega_s)$$

$$\mathbf{d}_L = \text{Re} \int_0^{\omega_p} \mathbf{c}_L(\omega) e^{j\omega k_{d2}} d\omega$$

$$= \begin{bmatrix} \frac{1}{k_{d2}} \sin k_{d2} \omega_p \\ \frac{1}{k_{d2}-1} \sin(k_{d2}-1)\omega_p \\ \vdots \\ \frac{1}{k_{d2}-N+1} \sin(k_{d2}-N+1)\omega_p \end{bmatrix}$$

ω_p and ω_s are the passband and stopband edges of G_0 , respectively, and $k_{d2} = k_d - k_{d1}$ is the group delay of G_0 . Obviously, the minimum point can be obtained as

$$\phi_L^* \text{opt} = -(\mathbf{V}_L^{*T} \mathbf{Q}_L \mathbf{V}_L^*)^{-1} \cdot (\mathbf{V}_L^{*T} \mathbf{Q}_L \mathbf{S}_{cL} - \mathbf{V}_L^{*T} \mathbf{d}_L) \quad (16)$$

and the coefficients of $G_0(z)$ are given by

$$\mathbf{g}_L^* = \mathbf{S}_{cL} + \mathbf{V}_L^* \phi_L^* \text{opt} \quad (17)$$

III. DESIGN EXAMPLES

We now present two design examples to illustrate the proposed algorithms. The related computer programs were written in MATLAB and run on a Sun SPARC station. The first example is to design a linear-phase perfect reconstruction QMF bank with design specifications $N = 20, M = 32$, and $\omega_s = 0.61\pi$. The analysis lowpass filter H_0 was first designed by the window method with passband and stopband edges 0.44π and 0.61π rad/s, respectively. The performance of the filter bank obtained is evaluated in terms of the peak-reconstruction error (PRE) defined by $\text{PRE} = \max_{\omega} |20 \log_{10} [|H_0(e^{j\omega})G_0(e^{j\omega}) - H_0(e^{j(\omega+\pi)})G_0(e^{j(\omega+\pi)})]|]$, and the signal-to-noise ratio (SNR) defined by

$$\text{SNR} = 10 \log_{10} \left(\frac{\text{energy of input signal}}{\text{energy of the reconstruction error}} \right)$$

$$= 10 \log_{10} \left\{ \frac{\sum x^2(n)}{\sum [x(n) - \hat{x}(n+k_d)]^2} \right\}$$

The SNR was calculated with a random input signal with a uniformly distributed amplitude. The results obtained are listed in Table I, and the amplitude responses of the analysis lowpass and highpass filters are depicted in Fig. 2.

The second example is a low-delay perfect reconstruction QMF bank with $N = 26, M = 34, k_d = 15, \omega_p = 0.45\pi, \omega_s = 0.65\pi$. The analysis lowpass filter H_0 was first designed by a least-squares approach with passband and stopband edges 0.5π and 0.65π rad/s, respectively, and $k_{d1} = 7.5$. The results obtained are given in Table I, and the amplitude responses of the

TABLE I
PERFORMANCE EVALUATIONS OF OBTAINED QMF BANKS

| | Example 1 | Example 2 |
|----------|------------------------|------------------------|
| PRE (dB) | 5.79×10^{-14} | 3.66×10^{-14} |
| SNR (dB) | 302 | 292 |

TABLE II
THE OUTPUTS OF EXP.1 AND EXP.2 WITH A RAMP INPUT

| n | $x(n)$ | Example 1 $\hat{x}(n+25)$ | Example 2 $\hat{x}(n+15)$ |
|-----|-------------------|------------------------------|------------------------------|
| 0 | 1.00000000000000 | 1.00000000000000 | 1.00000000000000 |
| 1 | 2.00000000000000 | 2.00000000000000 | 2.00000000000000 |
| 2 | 3.00000000000000 | 3.00000000000000 | 3.00000000000000 |
| 3 | 4.00000000000000 | 4.00000000000000 | 4.00000000000000 |
| 4 | 5.00000000000000 | 5.00000000000000 | 5.00000000000000 |
| 5 | 6.00000000000000 | 6.00000000000000 | 6.00000000000000 |
| 6 | 7.00000000000000 | 7.00000000000000 | 7.00000000000000 |
| 7 | 8.00000000000000 | 8.00000000000000 | 8.00000000000000 |
| 8 | 9.00000000000000 | 9.00000000000000 | 9.00000000000000 |
| 9 | 10.00000000000000 | 10.00000000000000 | 10.00000000000000 |

analysis lowpass and highpass filters are depicted in Fig. 3.

The performance of the obtained filter banks can also be checked by observing the output when the input is a ramp signal. As shown in Table II, for both examples the reconstructed signals were exactly the same as the input signal to within 13 significant digits after the decimal point.

IV. CONCLUSIONS

A new method for the design of linear-phase perfect reconstruction QMF banks has been proposed and it was then extended to the design of low-delay perfect reconstruction QMF banks. From the design example demonstrated it can be noted that the proposed method leads to perfect reconstruction in both the linear-phase and the low-delay cases.

REFERENCES

- [1] V. K. Jain and R. E. Crochiere, "Quadrature mirror filter design in the time domain," *IEEE Trans. Acoust., Speech, Signal Processing*, vol. ASSP-32, pp. 353-361, Apr. 1984.
- [2] C.-K. Chen and J.-H. Lee, "Design of quadrature mirror filters with linear phase in the frequency domain," *IEEE Trans. Circuits Syst.*, vol. 39, pp. 593-605, Sept. 1992.
- [3] T. Q. Nguyen and P. P. Vaidyanathan, "Two-channel perfect-reconstruction FIR QMF structures which yield linear-phase analysis and synthesis filters," *IEEE Trans. Acoust., Speech, Signal Processing*, vol. 37, pp. 466-690, May 1989.

- [4] B.-R. Horng, A. N. Willson, Jr., "Lagrange multiplier approaches to the design of two-channel perfect-reconstruction linear-phase FIR filter banks," *IEEE Trans. Signal Processing*, vol. 40, pp. 364-374, Feb. 1992.
- [5] H. Xu, W.-S. Lu, and A. Antoniou "A new approach for the design of FIR analysis-synthesis filter banks with short reconstruction delays," in *Proc. of Canadian Conf. on Elec. and Comp. Eng.*, pp. 31-34, Sept. 1993.

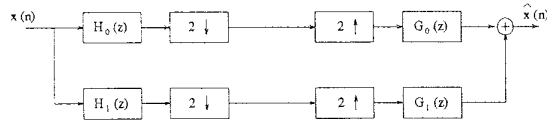


Fig. 1. Two-channel filter bank.

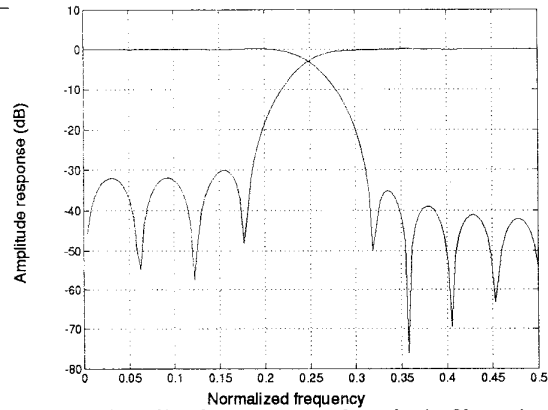


Fig. 2. Amplitude response of analysis filters in Example 1.

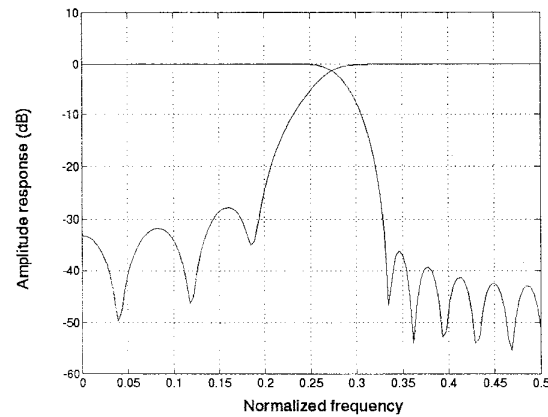


Fig. 3. Amplitude response of analysis filters in Example 2.